JOURNAL OF NANO- AND ELECTRONIC PHYSICS
Vol. **6** No 4, 04016(7pp) (2014)

ЖУРНАЛ НАНО- ТА ЕЛЕКТРОННОЇ ФІЗИКИ
Том **6** № 4, 04016(7cc) (2014)

Study of Elemental and Structural Phase Composition of Multilayer Nanostructured TiN / MoN Coatings, their Physical and Mechanical Properties

B.O. Postolnyi[1,*], P. Konarski[2], F.F. Komarov[3], O.V. Sobol'[4], O.V. Kyrychenko[1], D.S. Shevchuk[1]

[1] *Sumy State University, 2, Rymskogo-Korsakova Str., 40007 Sumy, Ukraine*
[2] *Tele and Radio Research Institute, 11, Ratuszowa Str., 03-450 Warszawa, Poland*
[3] *Belarusian State University, 4, Nezavisimosti Av., 220030 Minsk, Republic of Belarus*
[4] *National Technical University «Kharkiv Polytechnic Institute», 21, Frunze Str., 61002 Kharkiv, Ukraine*

(Received 01 September 2014; published online 29 November 2014)

This paper presents the results of investigation multilayer TiN / MoN coatings. Coatings were fabricated using Arc-PVD method. Period thickness of nanoscale layers in coatings was $\lambda = 8$, 25, 50 and 100 nm. The total thickness of coatings was up to 8.4 μm. Samples were studied using SEM, TEM, EDS, RBS, XRD, SIMS and nanoindentation. The actual thickness of the layers has a few larger values than expected (in most cases per 25 %). The formation of two phases was found: stoichiometric TiN (fcc) and cubic γ-Mo_2N (fcc). Maximum values of hardness and elasticity modulus were obtained for coating with $\lambda = 8$ nm: $H = 47$ GPa, $E = 470$ GPa. Plasticity index and its dependence on the thickness of layer period (λ) were calculated. The most plastic coating was the sample with $H / E = 0.1$.

Keywords: Nitrides, Nanostructured coatings, Multilayer, Wear resistance, Hardness, Elastic modulus, Plasticity index.

PACS numbers: 61.46. – w, 62.20. – x, 62.25. – g

1. INTRODUCTION

One of the most promising applications of nanomaterials is the creation of protective coatings for products and tools with different functional purposes. Such material characteristics as hardness, elasticity, adhesive and cohesive strength, durability, thermal and chemical stability and others are particularly important in this regard [1-15].

Results of scientific researches show the tendency of active use of nitrides and borides of transition metals and their combination in the development of protective materials. While nitrides of single elements are studied well enough, their multilayer modifications need more detailed study. Therefore the study of features of structure, elemental and phase composition of multilayer coatings depending on the deposition conditions is an important task in solid state physics and materials science.

2. EXPERIMENTAL DETAILS

Multilayer nanostructured TiN / MoN coatings were fabricated using vacuum arc evaporation of two cathodes at atmosphere of molecular nitrogen. For this procedure we used unit "Bulat-6", which allows obtaining coatings both for scientific purposes and for industry. Rotatable at predetermined speed substrate holder allows alternating deposition of titanium and molybdenum nitrides layers from two diametrically arranged evaporators [16]. Thus, it is possible to obtain coatings with different elemental and structural-phase compositions by adjusting the current and voltage of the substrate and cathodes, nitrogen pressure in the chamber and other parameters. The deposition parameters are located in Table 1.

Table 1 – Parameters of multilayer TiN/MoN deposition

Sample	Period λ, nm		t_{layer}, s	I_{dep}, A	I_{bias}, A	U_{bias}, V	f, kHz	p_N, Pa
	Expected	Measured						
# 1	4	8	2	95 ÷ 100	0.8	– 40	7	0.5
# 2	4	8				–230		
# 3	20	25	10		0.9	– 40		
# 4	20	25				–230		
# 5	40	50	20		0.9	– 40		
# 6	80	100	40		1.0	– 40		

Studies of the microstructure and the elemental composition of the coatings were carried out using a scanning electron microscope JEOL-7001F, also equipped with EDS microanalysis. SAED analysis was performed using transmission electron microscope JEOL 2200-FS equipped with a field-emission gun and omega energy filter. For full information about elemental composition of coatings Rutherford backscattering device (RBS) was used (on He^+ ions with an energy of 1.5 MeV, scattering angle $\theta = 170°$ at normal angle of ion incidence, detector energy resolution was 16 keV, He^+ dose was 5 μs). SIMS measurements were performed using SAJW-05 instrument with 500 nA, 1.72 keV Ar^+ primary ion beam at 45° incidence angle. Analyzer was equipped with Physical Electronics 06-350E ion gun and QMA-410 Balzers quadropole mass analyzer with 16 mm diameter rods. Structural-phase composition was studied using XRD analysis (Bruker Advanced 8 and DRON-4b) in Cu-K_α radiation. Measurements of hardness and Young's modulus were carried out on the equipment CSM Instruments.

* b.postolnyi@gmail.com

3. RESULTS AND DISCUSSION

As a result of deposition of samples the multi-layer coatings with various thicknesses of the individual layers from 8 to 100 nm were prepared. The total coating thickness was reached 8.4 microns.

The Fig. 1 shows a micrograph of a cross section of the sample # 6. Separate layers and coatings in general are clearly distinguished at selected magnification. Results of EDS analysis and coating composition (sample # 4) are shown in Fig. 2.

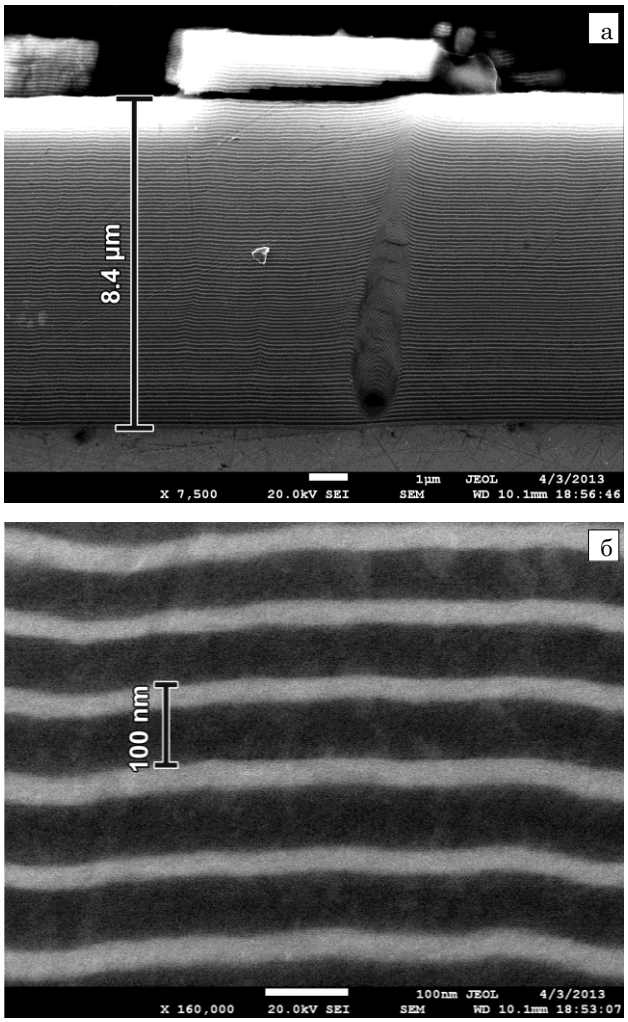

Fig. 1 – SEM images of multilayer TiN/MoN coating (sample # 6): a) the general view. The coating thickness is 8.4 μm, × 7 500 zoom; b) the cross-section fragment, × 50 000 zoom. Period λ = 100 nm

Energy spectra of Rutherford backscattering (RBS) give us more information about the structure and composition of the TiN/MoN coating.

The elemental composition of the samples was determined by RBS as well as EDS on cross-sectional images. RBS spectrum for TiN/MoN coatings with λ = 100 nm (sample # 3) is presented on the Fig. 3. The peaks in this spectrum correspond to all constituent elements of multilayer material. We can see kinematic factors for Ti and Mo at subsurface region of TiN/MoN coating. If we know it we can estimate the thickness of individual layer. Choosing number of channels and knowing the losses of ions on each of them, we can evaluate an average thickness of the layer on the cross-section of the analyzing beam. Using RBS spectrum data it is possible to estimate the thickness of the first four layers from the surface. According to the analysis, the thickness of MoN layer is ~ 10 nm. Regarding the TiN layer it was more than twice as large – approx. 19 nm.

Unfortunately, features of RBS analysis don't give us the opportunity to obtain information about the elemental composition of coating throughout its depth. Ion beam sputtering techniques are most often used for this [12, 17-20].

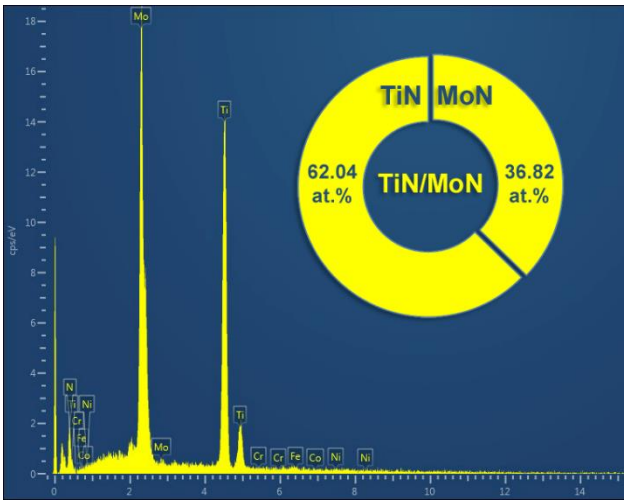

Fig. 2 – The energy-dispersive spectrum of coating (sample # 4)

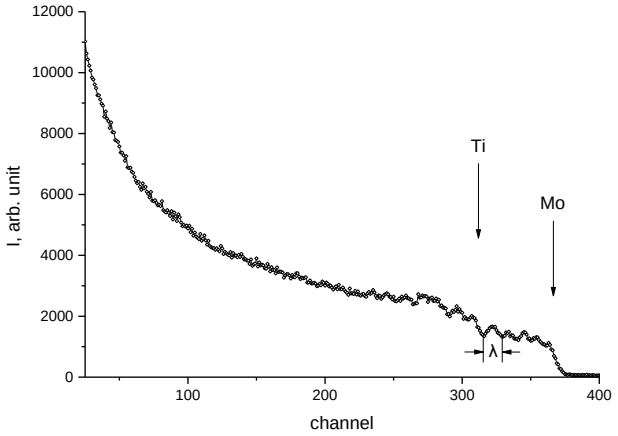

Fig. 3 – RBS spectrum for sample # 3

We used secondary ion mass spectroscopy (SIMS) for depth profile analysis in our work. Method based on sputtering of specimen using focused primary Ar^+ ion beam and gathering information about ejected secondary ions. It's should be noted that SIMS is destructive method of material investigation. During the depth profile analysis we sputtered the crater of 2.5 × 2.5 mm.

Prior to depth profile analysis we registered mass spectrum – see Fig. 4.

Preliminary results of depth profiling were registered for a set of m/z values: $m / z = 14$ (N^+), 16 (O^+), 28 (N_2^+), 48 (Ti^+), 62 (TiN^+), 98 (Mo^+) and 110 (Ti_2N^+). Results are shown in Fig. 5.

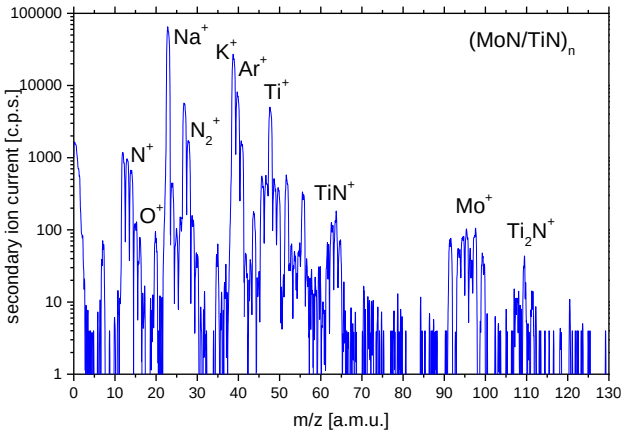

Fig. 4 – SIMS mass spectrum of positive secondary ions. Mass range 0-130 a.m.u

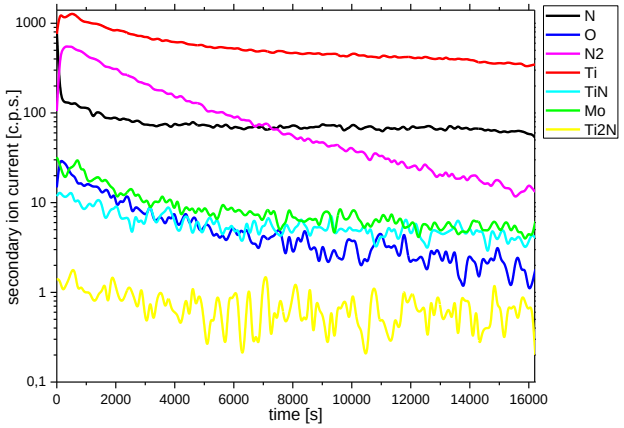

Fig. 5 – SIMS depth profile analysis of positive secondary ions: $m/z = 14$ (N^+), 16 (O^+), 28 (N_2^+), 48 (Ti^+), 62 (TiN^+), 98 (Mo^+) and 110 (Ti_2N^+). Time of analysis is 4.5 hours

Secondary ion currents of three masses $m/z = 14$ (N^+), 48 (Ti^+) and 98 (Mo^+) were considered in more detail (see Fig. 6). Relative ion currents can be extracted in two forms.

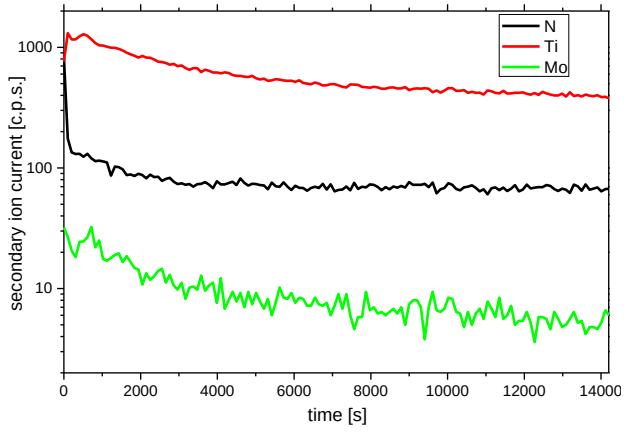

Fig. 6 – SIMS depth profile analysis of positive secondary ions: $m/z = 14$ (N^+), 48 (Ti^+) and 98 (Mo^+)

After smoothing the raw data and background subtraction we can present the data as a ratio of normalized ion currents to the sum of three normalized currents.

The obtained data were normalized using simple procedure, where the raw ion currents of each component (I_r) were multiplied by sensitivity factors (f), $I_r \times f = I_x$. The ratio of the I_x and the sum of all currents $I_x / \sum I_x$ may be treated as a rough indication of atomic concentration if we neglect the so called "matrix effect" [5, 6].

If we consider that the layer consists of the three elements and we assume TiN (1 : 1) and MoN (1 : 1) stoichiometry we obtain the data as presented below – Fig. 7. The layered structure of coatings is visible in both graphs (left and right).

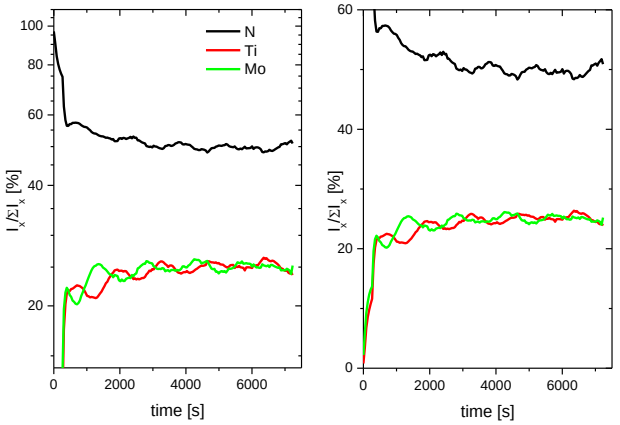

Fig. 7 – SIMS depth profile analysis of normalized secondary ion currents: $m/z = 14$ (N^+), 48 (Ti^+) and 98 (Mo^+). Logarithmic scale is on the left and linear scale – on the right

If we consider the presence of only two elements: Mo and Ti, we get the data shown in Fig. 8. The alternation of TiN and MoN layers is traced quite well in this graph. Unfortunately, surface roughness and relief layers of coating make it difficult to separate the layers more clearly by SIMS analysis.

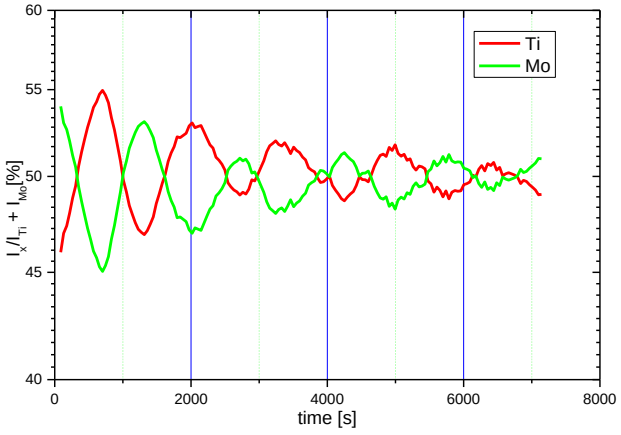

Fig. 8 – SIMS depth profile analysis of normalized secondary ion currents: $m/z = 48$ (Ti^+) and 98 (Mo^+)

Used parameters of depth profile analysis for sample # 4 lead to sputtering rate of 2.0 nm/min for SiO_2. Due to the roughness we didn't measure the crater depth with stylus profilometer.

In order to estimate the sputtering rate of TiN/MoN we carried out SRIM simulations (see Table 2). Most

likely that the sputtering rate of TiN and MoN was lower than for SiO_2 (lower than 2.0 nm/min). Having compared results of SRIM simulation with data obtained from RBS spectra and SEM-images of the cross-section of multilayer samples, we made the assumption that the average sputtering rate was about 1.1-1.3 nm/min (or ~0.02 nm/s).

Table 2 – Parameters of SIMS analysis and SRIM simulations

500 nA, 1.72 keV Ar^+ primary ion beam at 45° incidence angle			
Material	SiO_2	TiN	MoN
*S** (atoms/ion)	3.46	3.27	4.37
Ion range* (nm)	4.4	3.3	2.7
Sputtering rate (nm/min)	2.0	-	-

* Values obtained from SRIM simulation

The depth profile analysis was carried out for five hours. The crater of 2.5 × 2.5 mm was sputtered during this time. Taking as a basis sputtering rate 0.02 nm/s, it is possible to determine that crater depth was 360-400 nm. The Fig. 9 shows a modernized previous graph with the calculated thicknesses of the first few layers from the surface of TiN/MoN coating.

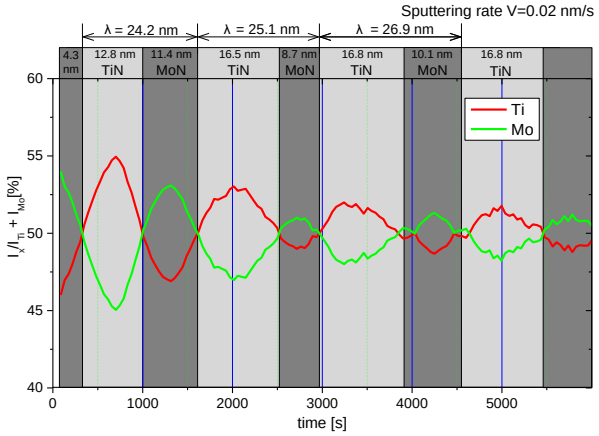

Fig. 9 – Determination of the coating layers based on SIMS analysis

XRD patterns of TiN/MoN multilayer coatings with double layer thickness of $\lambda = 25$, 50 and 100 nm are shown in Fig. 10. Main peaks are located around $2\theta = 36.5°$ and $2\theta = 42.5°$. A more detailed study of the spectral lines gave it possible to detect the asymmetric shape of the peaks.

Peaks found at $2\theta = 42.5°$ can be divided into two components, which correspond to (200) fcc TiN and (200) cubic γ-Mo_2N planes (see Fig. 11). The peak at $2\theta = 36.5°$ is attributed to (111)-oriented TiN and γ-Mo_2N grains. The volume fractions of TiN and γ-Mo_2N phases were extracted from the XRD line fitting procedure of (200) and (111) peaks using the "New_profile" software.

All of the identified peaks are marked in the Fig. 10. These results show that TiN/MoN coatings consist of highly-textured (200) cubic layers.

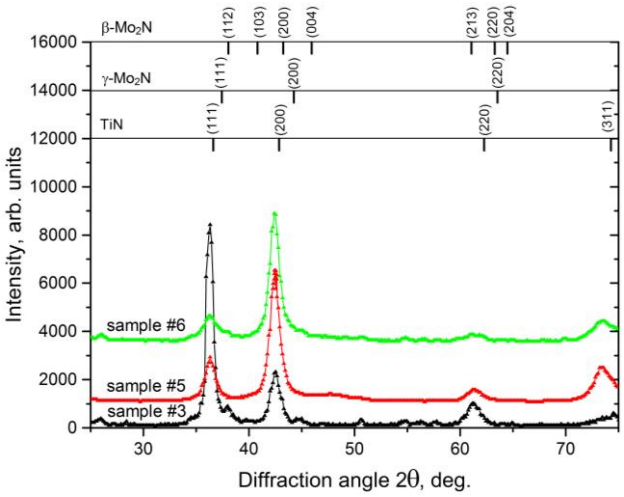

Fig. 10 – The diffraction patterns (XRD), obtained for coatings with different layer thickness $\lambda = 25$, 50 and 100 nm

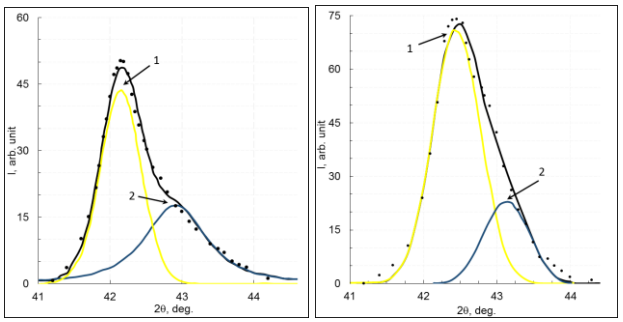

Fig. 11 – The separation of diffraction spectra into components peaks from the two phases: curve 1 – TiN (200); curve 2 – γ-Mo_2N (200). Sample # 5 – left, other – sample # 6

X-ray analysis shows the formation of only one phase with the fcc cubic lattice (structural type NaCl) in coating with $\lambda = 8$ nm when substrate voltage is - 40 V. The formation of two-phase system of TiN with NaCl-type fcc lattice and high temperature γ-Mo_2N is observed when substrate voltage is increasing to - 230 V. The volumetric ratio of TiN/γ-Mo_2N phases is 90/10 respectively.

The presence of only one phase at U_{bias} = - 40 V can be explained by the alleged epitaxial growth of thin layers, which growth period is determined by stronger bonds in TiN layer. Increasing of substrate potential to - 230 V leads to the appearance of two-phase as a result of intensification of ion bombardment, which contributes to the grain refinement and the beginning of interfaces formation. Formation of separate layers Mo_2N with a cubic lattice and the appearance of interphase boundaries leads to growth of stress in the TiN phase and an increase lattice period in unstressed section. The structure of these coatings is columnar.

The formation of two-phase structural state with cubic phases TiN and γ-Mo_2N with volume fraction 60 vol. % and 40 vol. % respectively is observed in coatings with $\lambda = 25$ nm. These XRD analysis data are well combined with EDS analysis data for values of Ti and Mo concentrations 62.3 at.% 36.8 at.% respectively (see Fig. 2 with EDS). Also more homogeneous surface morphology of the coating is typical for this series of

samples. Coatings which were obtained at less substrate potential (U_{bias} = - 40 V) have more smaller fractions than that obtained at U_{bias} = - 230 V.

For samples with thicker layers of titanium and molybdenum nitrides phase volume fraction accurately corresponds to the EDS analysis – 70 at.% TiN and 30 at.% Mo_2N. With increasing TiN/MoN layer thickness up to λ = 100 nm the growth of Mo_2N volume fraction up to 40 at. % is observed.

Fig. 12 shows TEM dark field image (sample # 5) which demonstrates columnar growth in multilayer nitride. It starts from interface between textured (111) steel substrate and TiN/MoN layers. Coating has a 100 nm thin internlayer which visible on TEM image and EDS mapping (Fig. 13). According to the data it consists of Ti, Mo, C and traces of N.

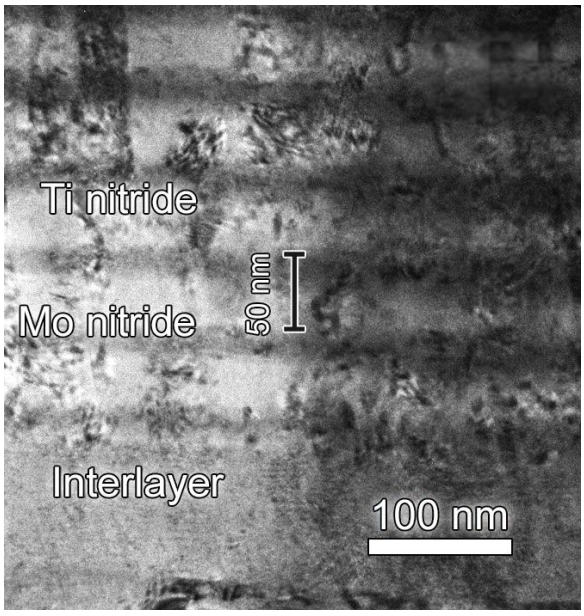

Fig. 12 – Cross-section TEM bright field image for sample # 5 with λ = 50 nm

Measurements of hardness and elasticity modulus of most samples were conducted to determine their mechanical properties and ability to durability. A more detailed study of hardness and elasticity are given for samples # 5 and # 6 in Fig. 14. They show typical regularities of H(L) and E(L). In measurements the indenter has reached a depth of coverage almost 3 μm. Penetration of the indenter was almost linear on the whole stage of load application.

Results of hardness and elasticity modulus measurements for coatings with different layer thicknesses are shown in Table 3. As seen, the hardness of the samples tends to decrease with growth of period λ in the coating. The maximum value of hardness was achieved at the minimum of the resulting coatings period λ = 8 nm – H = 47 GPa. Modulus of elasticity changed with changing the thickness of the double layer. The maximum value of E = 470 GPa was obtained at the same period λ = 8 nm.

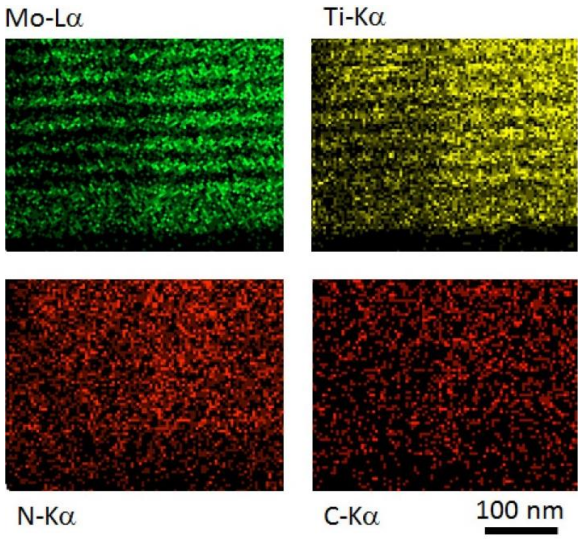

Fig. 13 – TEM-EDS chemical mapping for sample # 5

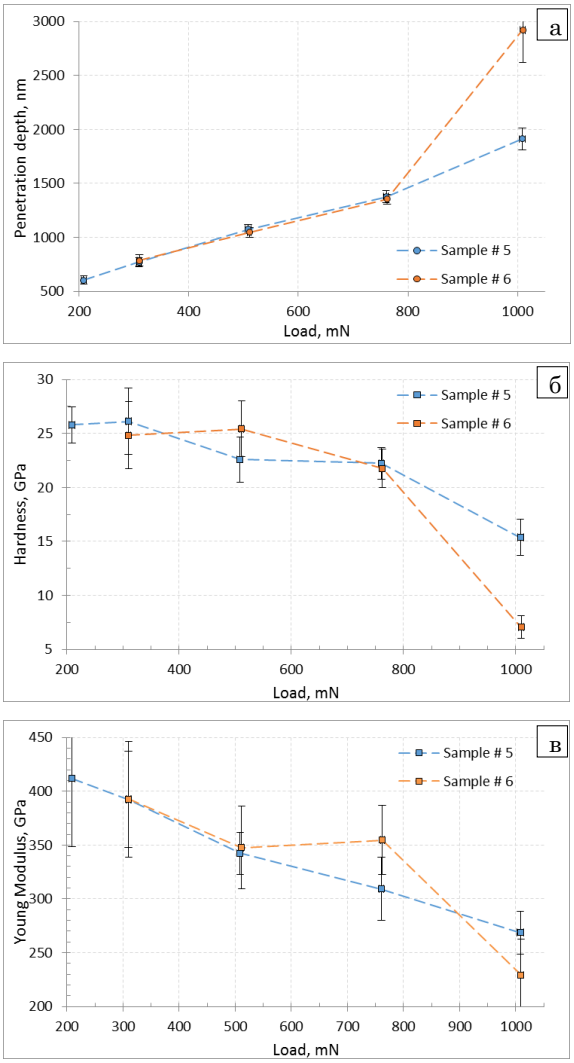

Fig. 14 – Physical and mechanical properties of coatings: dependence of penetration depth on the load (a), the hardness on the load (b) and Young modulus on the load (c)

Table 3 – Hardness and elasticity modulus measurements

λ, nm	H, GPa	E, GPa	H/E
8	47	470	0.1
25	31.8	456	0.07
50	26.5	418	0.063
100	25.4	392.6	0.065

However, knowing the values of hardness or elasticity of the material is not sufficient to predict its protective capacity [21-26]. The graph is shown in Fig. 15 which area is divided into sections: 1 – section with $H/E < 0.1$ which has no good plasticity of the material, 2 – section with good plasticity of the material. As can be seen, the sample # 2 with $\lambda = 8$ nm is flagged exactly on the line of plasticity.

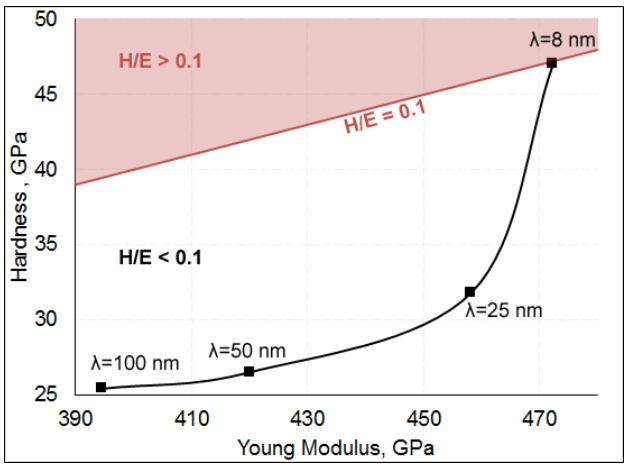

Fig. 15 – Characteristics of coatings plasticity

The general trend of graph testifies to expediency of the study multilayer TIN/MoN coatings at $\lambda \leq 8$ nm and at other thicknesses of layers.

These data indicate a good chance of producing TiN/MoN coatings with high plasticity and, hence, the wear resistance [18].

4. CONCLUSIONS

We have obtained multilayer nanostructured TiN/MoN coating which were not studied well by anyone else earlier. The elemental, structural and phase composition of coatings were studied. The thicknesses of the layers in the coating were measured in different ways and were slightly larger than the expected values. Total thickness values of coatings were reached 8.4 μm. Thicknesses of TiN/MoN period double layer were 8, 25, 50 and 100 nm. TiN layer thickness prevails over thickness of MoN in all obtained multilayer samples.

It was revealed that two-phase system coating with stoichiometric TiN (fcc) and cubic γ-Mo_2N (fcc) is forming during deposition. An interlayer of Mo, Ti, C and N was detected between substrate and multilayer TiN/MoN coatings.

Multi-layer coatings can be seen clearly in the SEM images of samples cross-sections, their TEM images, chemical mapping and other analysis methods. In addition, more detailed information about the subsurface layers of coatings we have obtained using SIMS depth profile analysis and RBS. Nanoindentation has allowed us to analyze the dependence of physical and mechanical properties of the coatings on their structural and phase composition and thickness of the layers, and, hence, to find the best conditions for obtaining protective coatings.

Also calculations for estimating plasticity and wear resistance of coatings were carried out. Best protective properties from the obtained materials possessed sample # 2 with $\lambda = 8$ nm. It has high values of hardness $H = 47$ GPa, modulus of elasticity $E = 470$ GPa, and plasticity index $H/E = 0.1$.

This indicates that the coating has good durability and resistance to wear. And multilayer coatings TiN/MoN have a prospect of further study, particularly at small thicknesses of layers in coating ($\lambda \leq 25$ nm and other).

AKNOWLEDGEMENTS

The authors would like to thank Prof. Alexander Pogrebnjak, Dr. Oleksandr Bondar (Sumy State University, Ukraine), Prof. Vyacheslav Beresnev (V.N. Karazin Kharkiv National University, Ukraine), Prof. Gregory Abadias, Dr. Patrick Chartier, Dr. Dominique Eyidi (University of Poitiers, France) for helping with the experiments and interpretation of results.

The work was carried out within the framework of Ukrainian comprehensive state program "Development of the basis for formation of multicomponent nanostructured superhard coatings with high physical and mechanical properties" (number 0112U001382) and "Physical principles of plasma technologies for complex processing of multicomponent materials and coatings" (number 0113U000137c).

Изучение элементного и структурно-фазового состава многослойных наноструктурных покрытий TiN/MoN, их физико-механические свойства

Б.А. Постольный[1], П. Конарский[1,2], Ф.Ф. Комаров[3], О.В, Соболь[4], Е.В. Кириченко[1], Д.С. Шевчук[1]

[1] *Сумский государственный университет, ул. Римского-Корсакова, 2, 40007 Сумы, Украина*
[2] *Теле-радио исследовательский институт, ул. Ратушова, 11, 03-450 Варшава, Польша*
[3] *Белорусский государственный университет, пр. Независимости, 4, 220001 Минск, Республика Беларусь*
[4] *НТУ "Харьковский Политехнический Институт", ул. Фрунзе, 21, 61002 Харьков, Украина*

В статье представлены результаты исследования многослойных покрытий TiN/MoN. Покрытия были получены с использованием вакуумно-дугового нанесения. Толщина периода наноразмерных слоёв в покрытиях составляла $\lambda = 8$, 25, 50 и 100 нм. Общая толщина покрытий составляла до 8.4 мкм. Образцы изучались с помощью РЭМ, ПЭМ, ЭДС, РОР, РСА, МСВИ и наноиндентирования. Фактические значения толщин образцов оказались несколько бóльшими ожидаемых (в большинстве случаев примерно на 25 %). Было обнаружено формирование двухфазной системы: стехиометрический TiN (ГЦК) и кубический γ-Mo_2N (ГЦК). Максимальные значения твёрдости и модуля упругости были получены для покрытия с $\lambda = 8$ нм: $H = 47$ ГПа, $E = 470$ ГПа. Были рассчитаны индекс пластичности и его зависимость от периода слоёв (λ). Наиболее пластичным покрытием оказался образец с $H/E = 0.1$.

Ключевые слова: Нитриды, Наноструктурные покрытия, Многослойный, Износостойкость, Твёрдость, Модуль упругости, Индекс пластичности.

Дослідження елементного й структурно-фазового складу багатошарових наноструктурних покриттів TiN/MoN, їх фізико-механічні властивості

Б.О. Постольний[1], П. Конарський[1,2], Ф.Ф. Комаров[3], О.В, Соболь[4], О.В. Кириченко[1], Д.С. Шевчук[1]

[1] *Сумський державний університет, вул. Римського-Корсакова, 2, 40007 Суми, Україна*
[2] *Теле-радіо дослідницький інститут, вул. Ратушова, 11, 03-450 Варшава, Польща*
[3] *Білоруський державний університет, пр. Незалежності, 4, 220001 Мінськ, Республіка Білорусь*
[4] *НТУ "Харківський Політехнічний Інститут", вул. Фрунзе, 21, 61002 Харків, Україна*

Ця стаття представляє результати дослідження багатошарових покриттів TiN/MoN. Покриття були отримані шляхом вакуумно-дугового нанесення. Товщина періоду нанорозмірних шарів у покритті складала $\lambda = 8$, 25, 50 і 100 нм. Загальна товщина покриттів складала до 8.4 мкм. Зразки досліджувалися за допомогою РЕМ, ПЕМ, ЕДС, РЗР, РСА, МСВІ та наноіндентування. Фактичні значення товщини зразків виявились дещо більшими за очікувані (у більшості випадків на 25 %). Було виявлено формування двофазної системи: стехіометричного TiN (ГЦК) і кубічного γ-Mo_2N (ГЦК). Максимальні значення твердості й модуля пружності були отримані для покриття з $\lambda = 8$ нм: $H = 47$ ГПа, $E = 470$ ГПа. Були розраховані індекс пластичності та його залежність від періоду шарів (λ). Найбільш пластичним покриттям виявився зразок з $H / E = 0.1$.

Ключові слова: Нітриди, Наноструктурні покриття, Багатошаровий, Зносостійкість, Твердість, Модуль пружності, Індекс пластичності.

REFERENCES

1. A.D. Pogrebnyak, Yu.N. Tyurin, *Phys.-Usp.* **48**, 487 (2005).
2. A.D. Pogrebnjak, A.P. Shpak, N.A. Azarenkov, V.M. Beresnev, *Phys.-Usp.* **52**, 29 (2009).
3. A.D. Pogrebnjak, S.N. Bratushka, V.M. Beresnev, N. Levintant-Zayonts, *Russ. Chem. Rev.* **82**, 1135 (2013).
4. P. Konarski, A. Mierzejewska, *Appl. Surf. Sci.* **203**, 354 (2003).
5. J.C. Reviere, S. Myhra, *Handbook of Surface and Interface Analysis* (New York: Marcel Dekker, Inc.: 1998).
6. P. Zalm, *Vacuum* **45**, 753 (1994).
7. P. Konarski, K. Kaczorek, M. Ćwil, J. Marks, *Vacuum* **81**, 1323 (2007).
8. A.D. Pogrebnjak, et al., *Mater. Chem. Phys.* **147**, 1079 (2014).
9. Y. Todaka, et al., *Rev. Adv. Mater. Sci.* **10**, 409 (2005).
10. A.D. Pogrebnjak, *J. Nanomater.* **2013**, 780125 (2013).
11. A.D. Pogrebnjak, A.G. Ponomarev, A.P. Shpak, *Phys.-Usp.* **55**, 270 (2012).
12. A.D. Pogrebnjak, V.M. Beresnev, *Nanocoatings Nanosystems Nanotechnologies* (Oak Park, IL: Bentham Science Publishers: 2012).
13. A.D. Pogrebnjak, V.M. Beresnev, A.A. Demianenko, *Phys. Solid State* **54**, 1882 (2012).
14. O. V. Sobol', et al, *Phys. Met. Metallogr.* **112**, 188 (2011).
15. V. Ivashchenko, et al., *Sci. Technol. Adv. Mater.* **15**, 025007 (2014).
16. A.D. Pogrebnjak, et al., *Tech. Phys. Lett.* **40**, 215 (2014).
17. A.D. Pogrebnyak, et al., *Tech. Phys.* **57**, 840 (2012).
18. J. Musil, *Surf. Coat. Technol.* **207**, 50 (2012).
19. M.K. Kazmanli, et. al., *Surf. Coat. Technol.* **167**, 77 (2003).
20. O.V. Bondar, et al. *CriMiCo 2013 - 2013 23rd International Crimean Conference Microwave and Telecommunication Technology, Conference Proceedings,* 865 (2013).
21. A.D. Pogrebnjak, et al., *Nucl. Instr. Meth. Phys. Res. B* **145**, 373 (1998).
22. A.D. Pogrebnjak, et al., *Surf. Coat. Technol.* **201**, 2621 (2006).
23. A.D. Pogrebnjak, et al., *Phys. Lett. A* **241**, 357 (1998).
24. A.D. Pogrebnjak, et al., *J. Friction Wear* **35**, 55 (2014).
25. A.D. Pogrebnjak, et al., *Proc. NAP* **2**, 02FNC27 (2013).
26. V.M. Beresnev, et al., *J. Friction Wear* **35**, 374 (2014).
27. B.O. Postolnyi, et al., *Proc. NAP* **3**, 01FNC06 (2014).